

High-temperature heat capacities and derived thermodynamic properties of anthophyllite, diopside, dolomite, enstatite, bronzite, talc, tremolite, and wollastonite

KENNETH M. KRUPKA¹

*Department of Geosciences
The Pennsylvania State University
University Park, Pennsylvania 16802*

BRUCE S. HEMINGWAY, RICHARD A. ROBIE

*U.S. Geological Survey
Reston, Virginia 22092*

AND DERRILL M. KERRICK

*Department of Geosciences
The Pennsylvania State University
University Park, Pennsylvania 16802*

Abstract

The heat capacities, C_p° , of magnesio-anthophyllite, diopside, dolomite, synthetic enstatite, bronzite, talc, tremolite and wollastonite have been determined to an accuracy of ± 1.0 percent by differential scanning calorimetry between 350 and 1000 K. The C_p° measurements for anthophyllite were also corrected to a composition of pure Mg-anthophyllite [$Mg_7Si_8O_{22}(OH)_2$]. These heat capacities were combined with existing low-temperature heat capacity, entropy, and high-temperature relative enthalpy data, and fitted by least squares to the following equations [T , in kelvin; C_p° , in J/(mol · K)]:

Magnesio-anthophyllite [$Mg_{6.3}Fe_{0.7}Si_8O_{22}(OH)_2$], (298–700 K)

$$C_p^\circ = 3287 - 1.628T - 1.885 \times 10^7 T^{-2} - 41859T^{-0.5} + 6.527 \times 10^{-4} T^2$$

Magnesio-anthophyllite [$Mg_7Si_8O_{22}(OH)_2$], (298–700 K)

$$C_p^\circ = 2713 - 0.9630T + 1.331 \times 10^7 T^{-2} - 33473T^{-0.5} + 2954 \times 10^{-4} T^2$$

Diopside [$CaMg(SiO_3)_2$], (298–1600 K)

$$C_p^\circ = 470.25 - 0.09864T + 2.453 \times 10^5 T^{-2} - 4823T^{-0.5} + 2.813 \times 10^{-5} T^2$$

Dolomite [$CaMg(CO_3)_2$], (298–650 K)

$$C_p^\circ = 547.9 - 0.1676T + 2.840 \times 10^6 T^{-2} - 6548T^{-0.5} + 7.708 \times 10^{-5} T^2$$

Enstatite (synthetic $MgSiO_3$), (298–1000 K)

$$C_p^\circ = 350.7 - 0.1473T + 1.679 \times 10^6 T^{-2} - 4296T^{-0.5} + 5.826 \times 10^{-5} T^2$$

Bronzite ($Mg_{0.85}Fe_{0.15}SiO_3$), (298–1000 K)

$$C_p^\circ = 207.9 - 0.01489T + 1.921 \times 10^5 T^{-2} - 2135T^{-0.5}$$

Talc [$Mg_3Si_4O_{10}(OH)_2$], (298–650 K)

$$C_p^\circ = 7963 - 7.513T + 6.505 \times 10^7 T^{-2} - 1.117 \times 10^5 T^{-0.5} + 3.806 \times 10^{-3} T^2$$

¹ Present address: Geosciences Research and Engineering Department, Battelle, Pacific Northwest Laboratories, Richland, Washington 99352.

Tremolite [$\text{Ca}_2\text{Mg}_5\text{Si}_8\text{O}_{22}(\text{OH})_2$], (298–800 K)

$$C_p^\circ = 6131 - 4.189T + 5.139 \times 10^7 T^{-2} - 8.566 \times 10^4 T^{-0.5} + 1.757 \times 10^{-3} T^2$$

Wollastonite (CaSiO_3), (298–1400 K)

$$C_p^\circ = 200.8 - 0.02590T - 1.579 \times 10^5 T^{-2} - 1826T^{-0.5} + 7.435 \times 10^{-6} T^2$$

By combining our calorimetric data with a high-temperature heat-of-solution value and ancillary thermodynamic data, we calculate $\Delta H_{f,298}^\circ$ and $\Delta G_{f,298}^\circ$ (based on the elements) for enstatite as -1549.60 ± 2.50 and -1462.10 ± 2.50 kJ/mol, respectively.

Introduction

The heat capacities for magnesio-anthophyllite, diopside, dolomite, enstatite, bronzite, talc, tremolite and wollastonite were measured between 350 and 1000 K using a differential scanning calorimeter (DSC). These minerals are important phases in the system $\text{CaO-MgO-SiO}_2\text{-H}_2\text{O-CO}_2$ and equilibria for the metamorphism of ultramafic rocks and siliceous dolomitic limestones. Diopside and enstatite are also important constituents in some igneous rocks. Our heat capacity, C_p° , data were combined with existing high-temperature relative enthalpy, $H_T^\circ - H_{298}^\circ$, data and new low-temperature C_p° and entropy, S_{298}° , data from Krupka et al. (1985) to derive high-temperature entropy and relative enthalpy values for these minerals. Prior to this study, high-temperature C_p° data and the derived thermodynamic properties, S_T° and $H_T^\circ - H_{298}^\circ$, were suspect or nonexistent for these minerals. Reliable values for S_T° are of critical importance to our understanding of metamorphic and igneous equilibria.

Materials

Differential scanning calorimeter (DSC) measurements were made on two samples of dolomite, $\text{CaMg}(\text{CO}_3)_2$. One sample was part of the material used in the experimental study of Slaughter et al. (1975). The second sample is from Binnental, Switzerland and was used by Stout and Robie (1963) for low-temperature heat capacity measurements. The preparation and chemical composition of these materials are described in Slaughter et al. (1975) and Stout and Robie (1963). Unit-cell dimensions were measured by the procedures described in Krupka (1984). The unit-cell dimensions for the Binnental dolomite sample are $a = 0.48078(4)$ and $c = 1.6008(3)$ nm. The other dolomite sample had the unit-cell dimensions $a = 0.48076(3)$ and $c = 1.6005(2)$ nm. These cell dimensions are in good agreement with the values in JCPDS pattern 11-78 and Goldsmith and Graf (1958) and compare favorably with the results of Goldsmith et al. (1961) for ordered dolomite.

The sample of talc, $\text{Mg}_3\text{Si}_4\text{O}_{10}(\text{OH})_2$, from Murphy, North Carolina, is the same material used in the low-temperature C_p° measurements of Robie and Stout (1963). The chemical composition of this material is described by Robie and Stout (1963). An X-ray pattern for this talc sample that contained a sufficient number of d -spacings with unique indices for a refinement of the unit-cell dimensions could not be obtained. An approximate value for the c -axis of 0.936 nm was obtained from five basal reflections in a pattern from a Guinier camera. This value is in agreement with the values $c = 0.9496$ nm from Rayner and Brown (1966, 1973) and $c = 0.9448$ nm from Ross et al. (1968).

Tremolite, $\text{Ca}_2\text{Mg}_5\text{Si}_8\text{O}_{22}(\text{OH})_2$, was obtained from two sources. One sample, from St. Gothard, Switzerland, was part of the material used by Slaughter et al. (1975), Eggert and Kerrick

(1981) and McKinstry and Skippen (1978). The second sample, from Falls Village, Connecticut,² was part of the material used for the C_p° measurements of Robie and Stout (1963). The chemical compositions of each sample are given in their respective references. The measured cell dimensions are $a = 0.9845(2)$, $b = 1.8055(3)$, $c = 0.52768(9)$ nm, and $\beta = 104^\circ 44.7'(9)$ for the sample from Falls Village, Connecticut, and $a = 0.9838(1)$, $b = 1.8049(2)$, $c = 0.52775(8)$, and $\beta = 104^\circ 45.1'(7)$ for the sample from St. Gothard, Switzerland. These cell dimensions are in good agreement with JCPDS files 13-437 and 20-1310, and with the tremolite data of Borg and Smith (1969).

The DSC samples of magnesio-anthophyllite, diopside, bronzite ($\text{Mg}_{0.85}\text{Fe}_{0.15}\text{SiO}_3$), synthetic enstatite (MgSiO_3), and wollastonite were aliquots of material used by Krupka et al. (1985) for low-temperature heat capacity measurements.

Apparatus and procedures

High-temperature heat capacities were measured with a Perkin-Elmer Model DSC-2³ differential scanning calorimeter. The measurements were made at a heating rate of 10 K/min and a range setting of 1.25 J/min (5 mcal/sec). The temperature interval between the initial and final temperatures for each DSC heating period was not more than 120 kelvins. An overlap of 40 kelvins was maintained between adjacent DSC scans as a check of the experimental precision. The masses of the DSC samples ranged from 24.9 to 34.3 mg.

A single crystal disc (30.660 mg) of Linde sapphire ($\alpha\text{-Al}_2\text{O}_3$) was used as the calorimetric standard. The heat capacity of $\alpha\text{-Al}_2\text{O}_3$ was taken from Ditmars and Douglas (1971). Temperature calibration of the calorimeter was monitored with measured transition temperatures (extrapolated onset temperature) of the inorganic compounds supplied in NBS-ICTA Standard Reference Materials 758 and 759 (McAdie et al., 1972). The estimated uncertainty for the DSC temperature measurements is ± 0.5 K.

Experimental results

The measured values of specific heat for magnesio-anthophyllite, diopside, dolomite, bronzite, synthetic enstatite, talc, tremolite, and wollastonite are listed in Tables 1 through 8, respectively. These data have not been corrected for deviations from their ideal end-member formulas. The experimental C_p° values are considered to be accu-

² Sample locality incorrectly listed as New York in Robie and Stout (1963).

³ The use of trade name is for descriptive purposes only and does not imply endorsement by Battelle, Pacific Northwest Laboratories, U.S. Geological Survey, or The Pennsylvania State University.

Table 1. High-temperature, experimental specific heats of natural anthophyllite

Temp. K	Specific heat J/(g·K)	Temp. K	Specific heat J/(g·K)	Temp. K	Specific heat J/(g·K)
349.90	0.9084	349.90	0.9112	510.00	1.0758
360.00	0.9161	359.90	0.9268	520.00	1.0845
370.00	0.9367	369.90	0.9404	530.00	1.0904
380.00	0.9430	379.90	0.9518	540.00	1.0977
390.00	0.9575	389.90	0.9635	550.00	1.1033
400.00	0.9695	399.90	0.9753	560.00	1.1101
410.00	0.9827	409.90	0.9867	570.00	1.1161
420.00	0.9937	419.90	0.9986	580.00	1.1219
430.00	1.0004	429.90	1.0093	590.00	1.1287
440.00	1.0155	439.90	1.0205	600.00	1.1352
425.00	0.9938	419.90	1.0000	580.00	1.1201
430.00	0.9965	429.90	1.0121	590.00	1.1232
440.00	1.0084	439.90	1.0226	600.00	1.1314
450.00	1.0197	449.90	1.0330	610.00	1.1385
460.00	1.0220	459.90	1.0425	620.00	1.1444
470.00	1.0326	469.90	1.0518	630.00	1.1483
480.00	1.0393	479.90	1.0609	639.90	1.1521
490.00	1.0508	489.90	1.0667	649.90	1.1555
500.10	1.0566	499.90	1.0741	659.90	1.1569
510.10	1.0745	509.90	1.0828	669.90	1.1615
520.10	1.0796	519.90	1.0887	679.90	1.1638
344.90	0.9042	500.00	1.0694		

rate to ±1.0%, based upon: (1) comparison of C_p° values in the temperature range 350–380 K determined by DSC analysis and low-temperature adiabatic calorimetry, and (2) the discussion by Krupka et al. (1979) concerning their DSC measurements for corundum and periclase. The average precision of the DSC measurements for the temperature range 350–1000 K is approximately 0.3%, but the precision degrades significantly to 0.5–1.0% above 850 K.

The experimental C_p° values for magnesio-anthophyllite were corrected to the ideal chemical compositions: $Mg_{6.3}Fe_{0.7}Si_8O_{22}(OH)_2$ and $Mg_7Si_8O_{22}(OH)_2$, using the same schemes as outlined in Krupka et al. (1985) for the low-temperature measurements on this anthophyllite. The differences between the C_p° values uncorrected and corrected to the ideal compositions are 0.6% for the Mg/Fe-anthophyllite and 3.0% for the pure Mg-anthophyllite. Heat capacity corrections for deviations from ideal chemical compositions were not applied to the data for the other minerals in this study because the corrections were significantly less than the uncertainty in the DSC measurements at high temperatures.

The heat capacities are shown graphically in Figures 1 through 4. For the sake of graphical clarity, approximately 50% of the C_p° values were omitted from these figures.

Specific heat values for magnesio-anthophyllite, diopside, bronzite, synthetic enstatite, and wollastonite, measured by DSC in the ranges 350–380 K, generally differed by less than 0.4% from the C_p° values measured by low-temperature adiabatic calorimetry (Krupka et al., 1985). Moreover, no differences were observed in the experimental C_p° values between the two samples of dolomite and

between the two samples of tremolite. Experimental C_p° measurements for diopside, bronzite, synthetic enstatite, and wollastonite were successfully completed over the full high-temperature range of the Perkin-Elmer DSC-2 (350–1000 K). Measurements for the other phases were terminated at lower temperatures due to apparent mineral decomposition reactions.

Heat capacity determinations for magnesio-anthophyllite were completed to a maximum temperature of 700 K. Above this temperature, the heating and isothermal sections of the DSC traces exhibited excessive and acceler-

Table 2. High-temperature, experimental specific heats of diopside

Temp. K	Specific heat J/(g·K)	Temp. K	Specific Heat J/(g·K)	Temp. K	Specific Heat J/(g·K)
360.10	0.8608	909.50	1.1189	369.90	0.8705
370.10	0.8714	929.40	1.1295	379.90	0.8806
390.10	0.8931	939.30	1.1378	389.90	0.8917
410.10	0.9125	949.20	1.1401	399.90	0.9032
430.10	0.9314	929.40	1.1318	409.90	0.9116
440.10	0.9416	939.30	1.1378	419.90	0.9217
420.00	0.9300	949.20	1.1291	429.90	0.9319
430.00	0.9337	959.10	1.1300	439.90	0.9388
450.00	0.9536	969.00	1.1443	419.90	0.9236
470.00	0.9697	958.90	1.1392	429.90	0.9328
490.00	0.9850	968.80	1.1323	439.90	0.9416
510.10	0.9951	978.70	1.1304	449.90	0.9467
520.10	0.9970	988.60	1.1314	459.90	0.9554
500.10	0.9905	998.40	1.1406	469.90	0.9628
510.10	0.9993	724.90	1.0796	479.90	0.9716
530.10	1.0090	729.90	1.0829	489.90	0.9781
550.10	1.0155	779.80	1.0926	499.90	0.9845
570.10	1.0233	799.80	1.1009	509.90	0.9919
590.10	1.0284	809.80	1.1018	519.90	0.9974
600.10	1.0362	724.90	1.0829	500.00	0.9868
580.20	1.0288	729.90	1.0870	510.00	0.9933
590.20	1.0349	739.80	1.0912	520.00	0.9998
610.20	1.0445	759.80	1.0935	530.00	1.0071
630.20	1.0487	779.80	1.1000	540.00	1.0122
650.00	1.0593	799.80	1.1064	550.00	1.0155
670.20	1.0690	809.80	1.1004	560.00	1.0205
680.20	1.0686	854.80	1.1143	570.00	1.0252
650.20	1.0681	859.80	1.1147	580.00	1.0284
660.20	1.0676	869.80	1.1157	590.00	1.0339
680.20	1.0759	889.80	1.1189	600.00	1.0358
700.20	1.0806	909.80	1.1267	580.00	1.0307
720.20	1.0898	919.80	1.1291	590.00	1.0381
730.20	1.0967	904.80	1.1309	600.00	1.0418
740.30	1.1004	909.80	1.1235	610.00	1.0464
720.20	1.0903	919.80	1.1291	620.00	1.0496
730.20	1.0935	939.80	1.1434	630.00	1.0538
750.30	1.0953	949.70	1.1540	639.90	1.0579
770.30	1.0953	929.80	1.1327	649.90	1.0616
790.30	1.0953	934.80	1.1291	659.90	1.0653
800.30	1.1055	939.80	1.1231	669.90	1.0718
760.30	1.0949	949.70	1.1194	679.90	1.0759
770.30	1.0995	959.70	1.1221	649.90	1.0621
780.30	1.1004	969.70	1.1498	659.90	1.0607
800.30	1.1041	960.00	1.1517	669.90	1.0704
810.30	1.1050	970.00	1.1461	769.90	1.0695
850.20	1.1134	980.00	1.1475	689.90	1.0732
860.10	1.1046	990.00	1.1411	699.90	1.0759
869.90	1.1060	999.90	1.1461	709.90	1.0833
889.70	1.1041	344.90	0.8418	719.90	1.0815
909.40	1.1180	349.90	0.8464	729.90	1.0833
919.30	1.1170	359.90	0.8594	739.90	1.0884
899.60	1.1166				

Table 3. High-temperature, experimental specific heats of dolomite

Temp.	Specific heat	Temp.	Specific heat	Temp.	Specific heat
K	J/(g·K)	K	J/(g·K)	K	J/(g·K)
350.10	0.9332	580.00	1.1431	519.90	1.1133
360.00	0.9446	590.00	1.1556	539.90	1.1263
380.00	0.9674	600.00	1.1702	559.90	1.1491
400.00	0.9967	349.70	0.9289	579.90	1.1599
420.00	1.0151	359.80	0.9403	589.90	1.1686
430.00	1.0276	379.80	0.9642	599.90	1.1783
440.00	1.0368	399.80	0.9902	534.80	1.1230
430.00	1.0308	419.90	1.0162	549.70	1.1247
440.00	1.0449	429.90	1.0260	569.70	1.1404
450.00	1.0525	439.90	1.0374	589.70	1.1496
470.00	1.0710	430.00	1.0308	609.70	1.1708
490.00	1.0856	440.00	1.0417	619.80	1.1854
509.90	1.1079	450.00	1.0515	534.80	1.1317
519.90	1.1133	470.00	1.0731	549.70	1.1371
510.00	1.1008	490.00	1.0862	569.70	1.1561
520.00	1.1046	509.90	1.1030	589.70	1.1670
540.00	1.1230	519.90	1.1122	609.70	1.1762
560.00	1.1355	509.90	1.1030	619.80	1.1876

Table 5. High-temperature, experimental specific heats of synthetic enstatite

Temp.	Specific heat	Temp.	Specific heat	Temp.	Specific heat
K	J/(g·K)	K	J/(g·K)	K	J/(g·K)
344.90	0.9015	530.00	1.0768	859.80	1.2193
349.90	0.9075	540.00	1.0828	869.80	1.2212
359.90	0.9214	550.00	1.0898	889.80	1.2342
369.90	0.9344	560.00	1.0957	909.80	1.2382
379.90	0.9463	570.00	1.1017	919.80	1.2382
389.90	0.9583	580.00	1.1077	904.80	1.2511
399.90	0.9712	590.00	1.1147	909.80	1.2501
409.90	0.9812	600.00	1.1196	919.80	1.2521
419.90	0.9931	580.00	1.1157	939.80	1.2481
429.90	1.0021	590.00	1.1196	949.70	1.2541
439.90	1.0101	600.00	1.1246	855.00	1.2302
419.90	0.9872	610.00	1.1286	860.00	1.2272
429.90	0.9981	620.00	1.1326	870.00	1.2332
439.90	1.0071	630.00	1.1356	890.00	1.2342
449.90	1.0141	639.90	1.1426	910.00	1.2412
459.90	1.0240	649.90	1.1465	920.00	1.2432
469.90	1.0320	659.90	1.1535	905.00	1.2412
479.90	1.0410	669.90	1.1615	910.00	1.2402
489.90	1.0479	679.90	1.1675	920.00	1.2402
499.90	1.0559	649.90	1.1445	940.00	1.2481
509.90	1.0639	659.90	1.1515	950.00	1.2581
519.90	1.0698	669.90	1.1535	930.00	1.2531
419.90	0.9872	679.90	1.1535	935.00	1.2581
429.90	0.9971	689.90	1.1625	940.00	1.2581
439.90	1.0071	699.90	1.1665	960.00	1.2661
449.90	1.0141	709.90	1.1734	970.00	1.2800
459.90	1.0250	719.90	1.1764	960.00	1.2591
469.90	1.0340	729.90	1.1834	970.00	1.2601
479.90	1.0429	739.90	1.1874	980.00	1.2571
489.90	1.0499	724.90	1.1724	990.00	1.2631
499.90	1.0559	729.90	1.1764	999.90	1.2591
509.90	1.0639	739.80	1.1794	960.00	1.2641
519.90	1.0708	759.80	1.1834	970.00	1.2621
500.00	1.0579	779.80	1.1894	980.00	1.2571
510.00	1.0639	799.80	1.1924	990.00	1.2491
520.00	1.0698	854.80	1.2143	999.90	1.2601

ating curvature in the endothermic direction. These results are consistent with the differential thermal analysis (DTA) measurements by Rabbitt (1948) for several samples of anthophyllite, and the 1 bar dehydration of anthophyllite estimated from the experimental studies of Greenwood (1963) and Chernosky and Autio (1979). Similar problems of de-

Table 4. High-temperature, experimental specific heats of bronzite

Temp.	Specific heat	Temp.	Specific heat	Temp.	Specific heat
K	J/(g·K)	K	J/(g·K)	K	J/(g·K)
425.00	0.9356	345.00	0.8457	630.10	1.0767
430.00	0.9404	350.00	0.8523	640.20	1.0824
440.00	0.9479	360.00	0.8646	650.20	1.0843
450.00	0.9517	370.00	0.8769	660.20	1.0919
460.00	0.9640	380.00	0.8873	670.20	1.0976
470.00	0.9754	390.00	0.9015	680.20	1.1023
480.00	0.9839	400.00	0.9120	650.20	1.0919
490.00	0.9943	410.00	0.9224	660.20	1.0957
500.10	1.0000	420.00	0.9318	670.20	1.0976
510.10	1.0142	430.00	0.9423	680.20	1.0995
520.10	1.0209	440.00	0.9517	690.20	1.1070
725.50	1.1184	500.20	1.0019	700.20	1.1099
730.20	1.1193	510.10	1.0095	710.20	1.1203
740.20	1.1203	520.10	1.0152	720.20	1.1260
750.20	1.1250	530.10	1.0237	730.20	1.1307
760.20	1.1279	540.20	1.0284	740.20	1.1317
770.20	1.1298	550.20	1.0341	900.80	1.1743
780.30	1.1373	560.20	1.0417	910.80	1.1752
790.30	1.1459	570.20	1.0493	920.80	1.1714
800.30	1.1478	580.20	1.0540	930.80	1.1781
855.30	1.1572	590.20	1.0597	940.80	1.1837
860.30	1.1591	600.20	1.0644	950.90	1.1961
870.30	1.1572	580.10	1.0540	960.90	1.1800
880.30	1.1610	590.10	1.0587	970.90	1.1875
890.30	1.1515	600.10	1.0635	980.90	1.1932
900.30	1.1610	610.10	1.0682	990.90	1.1942
910.30	1.1601	620.10	1.0758	1000.80	1.1970
920.40	1.1714				

hydration limited the high-temperature enthalpy determinations for amosite (fibrous ferro-anthophyllite) to 852 K by Bennington et al. (1978). The dolomite samples exhibited similar endothermic anomalies above 650 K. These results are in close agreement with the experimental data of Graf and Goldsmith (1955) for the thermal decomposition of dolomite in air.

Table 6. High-temperature, experimental specific heats of talc

Temp.	Specific heat	Temp.	Specific heat	Temp.	Specific heat
K	J/(g·K)	K	J/(g·K)	K	J/(g·K)
349.70	0.9536	490.00	1.1005	559.90	1.1487
359.80	0.9697	509.90	1.1123	579.90	1.1580
379.80	0.9992	519.90	1.1205	599.90	1.1698
399.80	1.0227	509.90	1.1147	609.90	1.1772
419.90	1.0425	519.90	1.1195	620.00	1.1701
429.90	1.0528	539.90	1.1287	564.90	1.1551
439.90	1.0588	559.90	1.1506	579.90	1.1619
430.00	1.0488	579.90	1.1595	589.90	1.1714
440.00	1.0591	589.90	1.1693	609.90	1.1838
450.00	1.0665	599.90	1.1732	629.90	1.1914
470.00	1.0876	544.90	1.1358	639.90	1.1986

Table 7. High-temperature, experimental specific heats of tremolite

Temp. K	Specific heat J/(g·K)	Temp. K	Specific heat J/(g·K)	Temp. K	Specific heat J/(g·K)
350.10	0.8936	660.00	1.1228	589.90	1.1030
360.00	0.9037	670.00	1.1247	599.90	1.1066
380.00	0.9272	680.00	1.1247	620.00	1.1146
400.00	0.9549	600.00	1.1297	640.00	1.1237
420.00	0.9729	720.00	1.1417	660.00	1.1303
430.00	0.9835	730.00	1.1503	670.00	1.1378
440.00	0.9936	740.00	1.1607	680.10	1.1399
530.00	0.9860	350.10	0.9063	660.00	1.1377
440.00	0.9981	360.00	0.9180	670.00	1.1392
450.00	1.0063	380.00	0.9389	680.00	1.1403
470.00	1.0228	400.00	0.9607	700.00	1.1478
490.00	1.0341	420.00	0.9816	720.00	1.1619
509.90	1.0544	430.00	0.9887	730.00	1.1716
519.90	1.0578	440.00	0.9968	640.00	1.1847
510.00	1.0485	430.00	0.9874	714.90	1.1531
520.00	1.0533	440.00	0.9951	729.90	1.1605
540.00	1.0672	450.00	1.0058	749.80	1.1641
560.00	1.0782	470.00	1.0257	769.80	1.1744
580.00	1.0901	490.00	1.0388	779.80	1.1742
590.00	1.0985	509.90	1.0538	789.80	1.1774
600.00	1.1086	519.90	1.0653	799.80	1.1857
589.90	1.0887	509.90	1.0497	714.90	1.1339
599.90	1.0927	519.90	1.0586	729.90	1.1324
620.00	1.0978	539.90	1.0719	749.80	1.1291
640.00	1.1077	559.90	1.0859	769.80	1.1444
660.00	1.1167	579.90	1.1007	779.80	1.1523
670.00	1.1284	589.90	1.1078	789.80	1.1588
680.10	1.1361	599.90	1.1113	799.80	1.1820

Table 8. High-temperature, experimental specific heats of wollastonite

Temp. K	Specific heat J/(g·K)	Temp. K	Specific heat J/(g·K)	Temp. K	Specific heat J/(g·K)
349.90	0.8075	439.90	0.8927	669.90	0.9908
360.00	0.8135	449.90	0.9013	689.90	0.9969
370.00	0.8264	459.90	0.9082	709.90	1.0055
380.00	0.8376	469.90	0.9151	729.90	1.0081
390.00	0.8445	479.90	0.9203	739.80	1.0141
400.00	0.8531	489.90	0.9237	725.00	1.0132
410.00	0.8669	499.90	0.9297	730.00	1.0132
420.00	0.8738	509.90	0.9357	740.00	1.0141
430.00	0.8763	519.90	0.9401	760.00	1.0115
440.00	0.8884	500.00	0.9246	780.00	1.0167
425.00	0.8781	510.00	0.9297	800.00	1.0330
430.00	0.8798	520.00	0.9357	810.00	1.0425
440.00	0.8867	530.00	0.9418	855.00	1.0485
450.00	0.8961	540.00	0.9461	860.00	1.0571
460.00	0.9005	550.00	0.9504	870.00	1.0571
470.00	0.9065	560.00	0.9564	890.00	1.0554
480.00	0.9099	570.00	0.9616	910.00	1.0520
490.00	0.9194	580.00	0.9650	920.00	1.0502
500.10	0.9228	590.00	0.9693	905.00	1.0563
510.10	0.9314	600.00	0.9745	910.00	1.0597
520.10	0.9332	580.00	0.9624	920.00	1.0640
344.90	0.8040	590.00	0.9667	940.00	1.0597
349.90	0.8083	600.00	0.9710	950.00	1.0545
359.90	0.8195	610.00	0.9745	930.00	1.0640
369.90	0.8290	620.00	0.9779	935.00	1.0657
379.90	0.8385	630.00	0.9796	940.00	1.0700
389.90	0.8479	639.90	0.9814	960.00	1.0743
399.90	0.8565	649.90	0.9848	970.00	1.0821
409.90	0.8652	659.90	0.9822	960.00	1.0778
419.90	0.8755	669.90	0.9865	970.00	1.0821
429.90	0.8841	679.90	0.9943	980.00	1.0838
439.90	0.8901	654.90	0.9840	990.00	1.0941
419.90	0.8755	659.90	0.9840	999.90	1.0761

The DSC measurements for talc and tremolite were likewise limited to 650 K and 800 K, respectively. According to the results described in Deer et al. (1971), the anomalous thermal behavior for talc is ascribed to the loss of adsorbed water from the fine-grained material. The maximum temperature for the talc measurements is approximately 150 degrees lower than the temperature obtained by extrapolating the results of Chernosky (1976) and Chernosky and Autio (1979) (where $P_{H_2O} = P_{Total}$) to 1 bar for the decomposition of talc. The thermal behavior of tremolite is similar to the results observed for magnesio-anthophyllite. The endothermic curvature in the DSC measurements on tremolite agrees with the stability limits for tremolite by Boyd (1959) when extrapolated to 1 bar.

Thermodynamic functions and heat capacity equations

Smoothed thermodynamic functions for magnesio-anthophyllite, diopside, dolomite, bronzite, synthetic enstatite, talc, tremolite, and wollastonite were calculated from a combination of: (1) high-temperature C_p^0 values from this study; (2) low-temperature C_p^0 data from Robie and Stout (1963), Stout and Robie (1963), and Krupka et al. (1985); and (3) the high-temperature relative enthalpy ($H_T^0 - H_{298}^0$) data in Southard (1941) and White (1919).

The DSC results were combined with low-temperature C_p^0 data (Krupka et al., 1985) and were fit over the range of

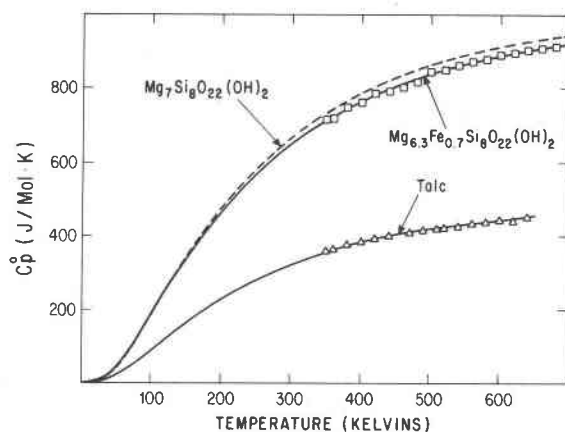


Fig. 1. Experimental high-temperature molar heat capacities of magnesio-anthophyllite (Mg_{6.3}Fe_{0.7}Si₈O₂₂(OH)₂) and talc. The solid curves from 0 to 298 K were taken from the results of low-temperature adiabatic calorimetry. The solid curves above 298 K were obtained from least-squares fits to the DSC data. The dashed curve represents the C_p^0 function for pure Mg-anthophyllite (Mg₇Si₈O₂₂(OH)₂) derived from impurity corrections to the experimental data for magnesio-anthophyllite.

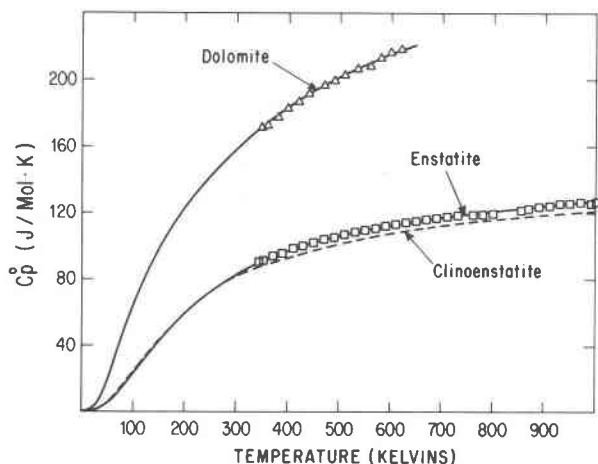


Fig. 2. Experimental high-temperature molar heat capacities of dolomite and synthetic enstatite (MgSiO_3). The solid curves from 0 to 298 K were taken from the results of low-temperature adiabatic calorimetry. The solid curves above 298 K were obtained from least-squares fits to the DSC data.

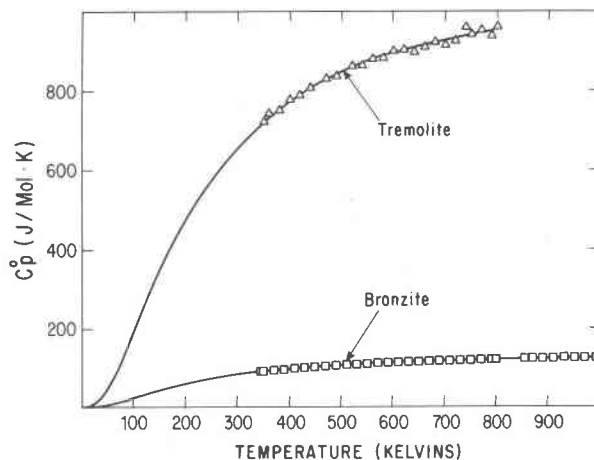


Fig. 4. Experimental high-temperature molar heat capacities of tremolite and bronzite ($\text{Mg}_{0.85}\text{Fe}_{0.15}\text{SiO}_3$). The solid curves from 0 to 298 K were taken from the results of low-temperature adiabatic calorimetry, whereas those above 298 K were obtained from least-squares fits to the experimental DSC data.

298 K to a maximal temperature of the data set by least squares, to an equation of the form

$$C_p^{\circ} = A + BT + CT^{-2} + DT^{-0.5} + ET^2, \quad (1)$$

as suggested by Haas and Fisher (1976). Only four terms of equation (1) were used if a fifth term made no significant contribution to the statistical fit, i.e., no significant decrease in the root mean square percent deviation. The fitting procedure constrained the C_p° at 298.15 K and the first deriva-

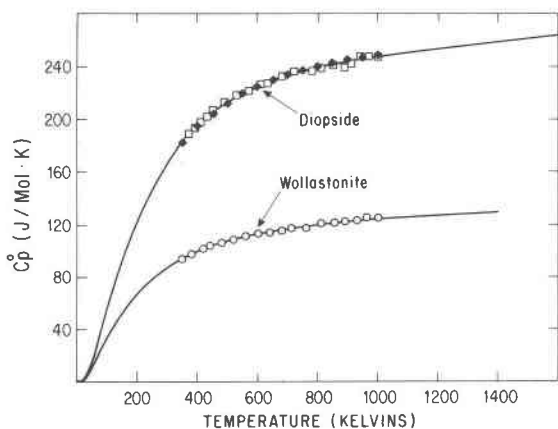


Fig. 3. Experimental high-temperature molar heat capacities of diopside and wollastonite. The open squares and open circles are the experimental DSC data for diopside and wollastonite, respectively. The solid diamonds are C_p° values for diopside derived from the equation given by Thompson et al. (1978). The solid curves from 0 to 298 K were taken from the results of low-temperature adiabatic calorimetry. The solid curves above 298 K were obtained from least-squares fits to the DSC data and selected drop calorimetric measurements referred to in the text.

tive of C_p° at 298.15 K to the values determined by low-temperature adiabatic calorimetry. This procedure insured that the high-temperature C_p° function smoothly joined with the data from low-temperature adiabatic calorimetry. The C_p° data determined by low-temperature adiabatic calorimetry were also weighted by a factor of two relative to the DSC values to further constrain the polynomial fits relative to the more accurate measurements.

The five-term C_p° equations for diopside and wollastonite were extended to 1600 and 1400 K, respectively, by incorporating the high-temperature relative enthalpy data of White (1919) for diopside and wollastonite, and those of Southard (1941) for wollastonite. The enthalpy data of White and Southard were recalculated to a reference temperature of 298.15 K and with the 1975 atomic weights. Their data were then combined with $H_T^{\circ} - H_{298}^{\circ}$ values computed from the DSC C_p° equations at temperatures at which DSC measurements were made, and fitted by least squares to the equation:

$$H_T^{\circ} - H_{298}^{\circ} = G + AT + (B/2)T^2 - CT^{-1} + 2DT^{0.5} + (E/3)T^3. \quad (2)$$

The fitting process retained the constraint that C_p° at 298.15 K had the values measured by low temperature adiabatic calorimetry, as well as the additional constraint that $H_T^{\circ} - H_{298}^{\circ} = 0$ at 298.15 K.

The final extended C_p° equations are given in Table 9. Errors in the derived thermodynamic functions are estimated to be $\pm 1.0\%$ in C_p° and $(H_T^{\circ} - H_{298}^{\circ})/T$, and $\pm 0.5\%$ in S_T° and $-(G_T^{\circ} - H_{298}^{\circ})/T$ between 298 and 1000 K. Tabulated values of the thermodynamic functions C_p° , $(H_T^{\circ} - H_{298}^{\circ})/T$, S_T° and $-(G_T^{\circ} - H_{298}^{\circ})/T$, derived from the equations in Table 9 are given in Krupka (1984).

Table 9. Molar heat capacity equations obtained by a least-squares fit of extended equation to experimental heat capacity data

Temperature range of equation	Average deviation between data and equation	Equations for C_p° in J/(mol·K) [Equation form from Haas and Fisher (1976)]
Magnesio-anthophyllite ($Mg_{6.3}Fe_{0.7}Si_8O_{22}(OH)_2$) (298 - 700 K)	0.4	$C_p^{\circ} = 3286.7 - 1.6275T + 1.8846 \times 10^7 T^{-2} - 41859T^{-0.5} + 6.5265 \times 10^{-4} T^2$
Magnesio-anthophyllite ^a ($Mg_7Si_8O_{22}(OH)_2$) (298 - 700 K)	0.4	$C_p^{\circ} = 2713.2 - 0.96304T + 1.3306 \times 10^7 T^{-2} - 33473T^{-0.5} + 2.9545 \times 10^{-4} T^2$
Diopside ($CaMg(SiO_3)_2$) (298 - 1000 K) (298 - 1600 K)	0.3	$C_p^{\circ} = 931.07 - 0.46366T + 6.8103 \times 10^6 T^{-2} - 12386T^{-0.5} + 1.6535 \times 10^{-4} T^2$ $C_p^{\circ} = 470.25 - 0.098644T + 2.4535 \times 10^5 T^{-2} - 4822.6T^{-0.5} + 2.8129 \times 10^{-5} T^2$
Dolomite ($CaMg(CO_3)_2$) (298 - 650 K)	0.4	$C_p^{\circ} = 547.88 - 0.16759T + 2.8400 \times 10^6 T^{-2} - 6547.9T^{-0.5} + 7.7076 \times 10^{-5} T^2$
Enstatite (synthetic $MgSiO_3$) (298 - 1000 K)	0.3	$C_p^{\circ} = 350.68 - 0.14725T + 1.6789 \times 10^6 T^{-2} - 4295.7T^{-0.5} + 5.8264 \times 10^{-5} T^2$
Bronzite ($Mg_{0.85}Fe_{0.15}SiO_3$) (298 - 1000 K)	0.3	$C_p^{\circ} = 207.93 - 0.014888T + 1.9207 \times 10^5 T^{-2} - 2135.3T^{-0.5}$
Talc ($Mg_3Si_4O_{10}(OH)_2$) (298 - 650 K)	0.4	$C_p^{\circ} = 7962.7 - 7.5132T + 6.5047 \times 10^7 T^{-2} - 1.1174 \times 10^5 T^{-0.5} + 3.8061 \times 10^{-3} T^2$
Tremolite ($Ca_2Mg_5Si_8O_{22}(OH)_2$) (298 - 800 K)	0.6	$C_p^{\circ} = 6131.0 - 4.1890T + 5.1385 \times 10^7 T^{-2} - 8.5656 \times 10^4 T^{-0.5} + 1.7568 \times 10^{-3} T^2$
Wollastonite ($CaSiO_3$) (298 - 1000 K) (298 - 1400 K)	0.3	$C_p^{\circ} = 438.55 - 0.22653T + 2.9355 \times 10^6 T^{-2} - 5624.2T^{-0.5} + 8.8565 \times 10^{-5} T^2$ $C_p^{\circ} = 200.80 - 0.025898T - 1.5789 \times 10^5 T^{-2} - 1826.4T^{-0.5} + 7.4346 \times 10^{-6} T^2$

^a Corrected for impurities to pure end-member composition.

^b Extended beyond 1000 K using drop-calorimetric measurements.

These DSC results and the low-temperature C_p° data were also fit by least squares to the equation:

$$C_p^{\circ} = A + BT + CT^{-2}, \quad (3)$$

suggested by Maier and Kelley (1932). The Maier-Kelley C_p° equations for magnesio-anthophyllite (Mg/Fe and pure Mg compositions), diopside, dolomite, bronzite, synthetic enstatite, talc, tremolite, and wollastonite are given in Table 10. The results in Tables 9 and 10 indicate that the five-term C_p° equation provides a superior fit to the data when compared to that obtained by the Maier-Kelley equation. When the extended C_p° equation was used, the percent deviation between the calculated and measured C_p° values was less than the experimental precision. The average percent deviations between the experimental values and C_p° values calculated from the Maier-Kelley equation, however, are greater than the precision of the measure-

ments and are 2-5 times greater than those computed from the extended equation.

Heat capacity and entropy values at several selected temperatures have been calculated from the extended C_p° equations (Table 9) and compared with similar values calculated from the Maier-Kelley equations (Table 10). The comparison of these two sets of data are shown in Table 11. Note that some of the differences between the two sets of C_p° and S_T° values are significant. It has been shown that the extended, five-term C_p° equation (equation 1) provides a superior fit to quantitative C_p° data. However, extrapolations using the extended C_p° equation beyond the temperature limits used in fitting are not valid physically. On the other hand, the Maier-Kelley equation (equation 3) can usually be extrapolated with a fair predictability for a short temperature range. This predictable behavior is due to the decreasing contribution of the CT^{-2} term as temperature increases, thus limiting the Maier-Kelley C_p° equation to

Table 10. Molar heat capacity equations obtained by a least-squares fit of Maier-Kelley C_p^0 equation to experimental heat capacity data

Temperature range of equation	Average deviation between data and equation	Equations for C_p^0 in J/(mol·K) [Equation form from Maier and Kelley (1932)]
Magnesio-anthophyllite ($Mg_{6.3}Fe_{0.7}Si_8O_{22}(OH)_2$) (298 - 700 K)	0.8	$C_p^0 = 648.1 + 0.4663T - 1.244 \times 10^{-7}T^{-2}$
Magnesio-anthophyllite ^a ($Mg_7Si_8O_{22}(OH)_2$) (298 - 700 K)	0.8	$C_p^0 = 670.5 + 0.4711T + 1.3105 \times 10^{-7}T^{-2}$
Diopside ($CaMg(SiO_3)_2$) (298 - 1600 K)	0.7 ^b	$C_p^{0c} = 220.1 + 0.03245T - 5.597 \times 10^{-6}T^{-2}$
Dolomite ($CaMg(CO_3)_2$) (298 - 650 K)	0.6	$C_p^0 = 141.5 + 0.1359T - 2.175 \times 10^{-6}T^{-2}$
Enstatite (synthetic $MgSiO_3$) (298 - 1000 K)	1.5	$C_p^0 = 90.11 + 0.04133T - 1.811 \times 10^{-6}T^{-2}$
Bronzite ($Mg_{0.85}Fe_{0.15}SiO_3$) (298 - 1000 K)	1.4	$C_p^0 = 89.93 + 0.04159T - 1.808 \times 10^{-6}T^{-2}$
Talc ($Mg_3Si_4O_{10}(OH)_2$) (298 - 650 K)	1.2	$C_p^0 = 314.8 + 0.2488T - 5.979 \times 10^{-6}T^{-2}$
Tremolite ($Ca_2Mg_5Si_8O_{22}(OH)_2$) (298 - 800 K)	1.9	$C_p^0 = 661.4 + 0.4203T - 1.166 \times 10^{-7}T^{-2}$
Wollastonite ($CaSiO_3$) (298 - 1400 K)	0.7 ^b	$C_p^{0c} = 108.5 + 0.01800T - 2.463 \times 10^{-6}T^{-2}$

^a Corrected for impurities to pure end-member composition.
^b Deviation calculated just for DSC C_p^0 values.
^c Extended beyond 1000 K using drop-calorimetric measurements.

essentially a linear equation. However, the slope of the C_p^0 equation may be significantly different from that of the measured heat capacity data at the high-temperature limit of the data.

Comparison with previous studies

Drop calorimetric measurements of relative enthalpy between 273 and 1373 K have been made by White (1919) for a sample labeled as "magnesium metasilicate in the amphibole form." The nature of this sample cannot be verified because White (1919) provides no additional characterization of the sample. However, the measurements by White (1919) should be mentioned because they have been the single source of high-temperature C_p^0 data for earlier thermochemical studies of anthophyllite equilibria (Day and Halbach, 1979, p. 814). Three-term Maier-Kelley C_p^0 equations have been fit to the drop calorimetric measurements of White (1919) and are listed in Goranson (in Birch et al., 1942, p. 230) and Kelley (1960). Heat capacity values tabulated in Barin et al. (1977, p. 389) for

anthophyllite are based on Goranson's C_p^0 equation. However, we could not locate the source of the value $S_{298}^0 = 559.0$ J/(mol·K) for anthophyllite given in Barin et al. (1977). Without additional mineralogical characterization, the measurements of White (1919) for a "magnesium silicate in the amphibole form" have limited value.

The high-temperature C_p^0 of diopside has been previously determined by Thompson et al. (1978), Wagner (1932), and White (1919). The C_p^0 equation reported by Thompson et al. (1978) covers the temperature range 350–1000 K, and was measured with a DSC identical to the instrument used in this study. Heat capacity values calculated from their equation at 50 degree intervals are shown in Figure 3. The maximum difference between their smooth C_p^0 values and those determined in this study is 0.8%, which is less than the experimental uncertainty.

Wagner (1932) and White (1919) used high-temperature drop calorimetry to measure the relative enthalpy (heat content) of diopside between 273 and 1573 K. Their enthalpy data were recomputed to values of the mean heat

Table 11. Comparison of heat capacity and entropy values computed from the extended C_p^0 equations (Table 9) with those calculated from the Maier-Kelley C_p^0 equations (Table 10).

Thermodynamic Property	C_p^0 and S_T^0 Values in J/(mol·K)							
	Mg-Fe-anthophyllite		Diopside		Dolomite		Bronzite	
	$T_{max} = 700$ K		$T_{max} = 1600$ K		$T_{max} = 650$ K		$T_{max} = 1000$ K	
	Table 9	MK Eq. ^a	Table 9	MK Eq. ^a	Table 9	MK Eq. ^a	Table 9	MK Eq. ^a
C_p^0 (550 K)	866.4	863.5	200.4	219.4	209.2	209.0	109.3	106.8
C_p^0 (T_{max})	923.5	949.1	310.8	269.8	221.4	224.6	125.7	129.7
S_T^0 (550 K)	1007	1004	262.4	263.4	268.0	267.4	128.1	127.4
S_T^0 (T_{max})	1224	1222	530.3	524.3	303.9	303.6	198.9	197.8
	Enstatite, synthetic		Talc		Tremolite		Wollastonite	
	$T_{max} = 1000$ K		$T_{max} = 650$ K		$T_{max} = 800$ K		$T_{max} = 1400$ K	
	Table 9	MK Eq. ^a	Table 9	MK Eq. ^a	Table 9	MK Eq. ^a	Table 9	MK Eq. ^a
C_p^0 (550 K)	109.7	106.9	432.5	431.9	876.0	854.1	110.4	110.3
C_p^0 (T_{max})	127.5	129.6	458.6	462.4	956.0	979.5	130.2	132.5
S_T^0 (550 K)	125.6	124.7	496.0	492.5	1023	1014	142.5	142.9
S_T^0 (T_{max})	196.6	195.0	570.2	567.1	1367	1356	255.9	256.2

^a MK Eq. = Values calculated from Maier-Kelley C_p^0 equations in Table 10 and S_{298}^0 values determined from low-temperature C_p^0 measurements.

capacity, $(H_T^0 - H_{298}^0)/(T - 298)$, and the 1975 values for the atomic weights, and plotted in Figure 5 along with analogous values derived from the DSC C_p^0 equation for diopside in Table 9. Mean heat capacity values, as opposed to $H_T^0 - H_{298}^0$ values, provide a more sensitive method for comparing different sets of enthalpy values and measured C_p^0 values (Douglas and King, 1968). Wagner's values, except for his data at 571 K, are lower than the values derived from the DSC measurements by 1 to 2%. The data of White (1919) are in closer agreement with the DSC values and differ by less than 0.5% from the values determined in this study. The two sets of drop calorimetric measurements are only in accord above 1300 K.

Leonidov and Khitarov (1967) report heat capacity values for talc from 373 to 1073 K determined by thermal analysis to an accuracy of $\pm 2\%$. Their smooth C_p^0 values for the temperature range 400–650 K differ from those determined in this study by 1.0–2.2%. Although these differences are within the experimental uncertainty stated by Leonidov and Khitarov, the composition of their talc sample differs somewhat from the ideal talc formula.

High-temperature heat contents of wollastonite have been measured by drop calorimetry between 300 and 1500 K by von Gronow and Schwiete (1933), Roth and Bertram

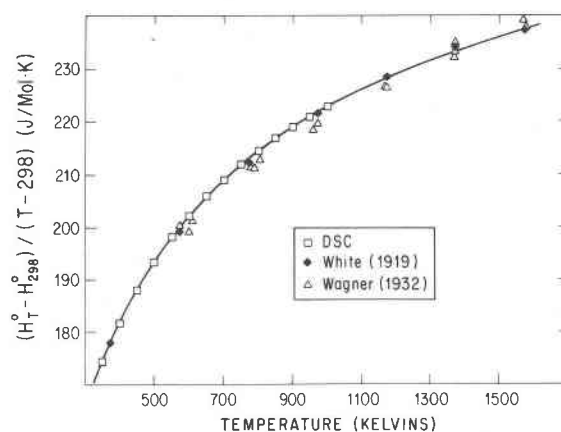


Fig. 5. Plot of mean heat capacity $(H_T^0 - H_{298}^0)/(T - 298)$ versus T to compare DSC C_p^0 data for diopside against heat content data determined by drop calorimetry. The open squares are values derived from the C_p^0 equation for diopside determined in this study by DSC analysis. The solid diamonds and open triangles are the drop calorimetric data of White (1919) and Wagner (1932), respectively. The solid curve is a least-squares fit to the DSC data and the drop calorimetric data of White (1919) above 1000 K.

(1929), Southard (1941), Wagner (1932) and White (1919). Except for the data of Roth and Bertram (1929), which are lower than all other data by 1 to 2 percent, the drop measurements are in good agreement with the DSC-derived values between 350 to 1000 K. Above 1000 K, the data of Southard (1941) and White (1919) are in accord with each other, and are several percent higher than the values of Roth and Bertram (1929) and Wagner (1932).

$\Delta H_{f,298}^{\circ}$ and $\Delta G_{f,298}^{\circ}$ for enstatite

Charlu et al. (1975) determined the enthalpies of solution at 970 K for three samples of enstatite using molten-oxide solution calorimetry. Using the average of three $\Delta H_{s,970}^{\circ}$ values for enstatite and their $\Delta H_{s,970}^{\circ}$ values for MgO and SiO₂, Charlu et al. (1975) obtained $\Delta H_{r,970}^{\circ} = -36.94 \pm 0.71$ kJ/mol (-8.83 ± 0.17 kcal/mol) for the reaction $\text{MgO} + \text{SiO}_2 = \text{MgSiO}_3$. Charlu et al. (1975, Table 2) actually report $\Delta H_{r,970}^{\circ}$ to be -8.81 ± 0.17 kcal/mol; this value, however, seems to be a typographical error based upon a review of the reported heats of solution.

Because S_{298}° and high-temperature C_p° values for enstatite were nonexistent at the time of their study, Charlu et al. could not compute $\Delta H_{f,298}^{\circ}$ and $\Delta G_{f,298}^{\circ}$ for enstatite. Using our high-temperature C_p° data, the entropy for enstatite at 298.15 K from Krupka et al. (1985), and ancillary data in Robie et al. (1979), we calculate $\Delta H_{f,298}^{\circ}$ and $\Delta G_{f,298}^{\circ}$ (from the oxides) for enstatite as -37.38 ± 2.27 and -36.74 ± 2.27 kJ/mol, respectively. Values for $\Delta H_{f,298}^{\circ}$ and $\Delta G_{f,298}^{\circ}$ for enstatite based on the elements are $-1,549.60 \pm 2.50$ and $-1,462.10 \pm 2.50$ kJ/mol, respectively.

Acknowledgments

This paper is partly based on K. M. Krupka's Ph.D. research at The Pennsylvania State University. The authors are particularly grateful to Profs. Bernard W. Evans and Peter Misch at the University of Washington for providing the anthophyllite sample, to Prof. Jun Ito (deceased) of the University of Chicago for providing the sample of synthetic enstatite, and to J. Stephen Huebner at the U.S. Geological Survey, Reston, Va., for providing the bronzite sample. We are also grateful to John L. Haas, Jr., Henry T. Hazelton, Jr., Susan W. Kieffer, and Donald E. Voigt, all of the U.S. Geological Survey, and Bruce D. Velde at Ecole Normale Supérieure, Paris, France, for critically reviewing the manuscript and providing helpful comments. This work was supported by the U.S. Geological Survey and by grants EAR 76-84199 and EAR 79-08244 from the Earth Sciences Division of the National Science Foundation to D. M. Kerrick. We also thank the Battelle, Pacific Northwest Laboratory for providing funds for the preparation of this manuscript.

References

- Barin, I., Knacke, O., and Kubaschewski, O. (1977) *Thermochemical Properties of Inorganic Substances (Supplement)*. Springer-Verlag, New York.
- Bennington, K. O., Ferrante, M. J. and Stuve, J. M. (1978) *Thermodynamic data on the amphibole asbestos minerals amosite and crocidolite*. U.S. Bureau of Mines Report of Investigations 8265.
- Birch, R., Schairer, J. F., and Spicer, H. C. (1942) *Handbook of Physical Constants*. Geological Society of America Special Paper 36.
- Borg, I. Y. and Smith, D. K. (1969) *Calculated X-ray Powder Patterns for Silicate Minerals*. Geological Society of America, Memoir 122.
- Boyd, F. R. (1959) *Hydrothermal investigations of amphiboles*. In P. H. Abelson, Ed., *Researches in Geochemistry*, Volume 1, p. 377-396. John Wiley and Sons, New York.
- Charlu, T. V., Newton, R. C., and Kleppa, O. J. (1975) *Enthalpies of formation at 970 K of compounds in the system MgO-Al₂O₃-SiO₂ from high temperature solution calorimetry*. *Geochimica et Cosmochimica Acta*, 39, 1487-1497.
- Chernosky, J. V., Jr. (1976) *The stability of anthophyllite—a re-evaluation based on new experimental data*. *American Mineralogist*, 61, 1145-1155.
- Chernosky, J. V., Jr., and Autio, L. K. (1979) *The stability of anthophyllite in the presence of quartz*. *American Mineralogist*, 64, 294-303.
- Darken, L. S. and R. W. Gurry (1953) *Physical Chemistry of Metals*. McGraw-Hill, New York.
- Day, H. W. and Halback, H. (1979) *The stability field of anthophyllite: the effect of experimental uncertainty on permissible phase diagram topologies*. *American Mineralogist*, 64, 809-823.
- Deer, W. A., Howie, R. A., and Zussman, J. (1971) *Rock Forming Minerals: Vol. 3 Sheet Silicates*. Longman Group Limited, London.
- Ditmars, D. A. and Douglas, T. B. (1971) *Measurement of the relative enthalpy of pure α -Al₂O₃ (NBS heat capacity and enthalpy standard reference material no. 720) from 273 to 1173 K*. U.S. National Bureau of Standards Journal of Research, 75A, 401-420.
- Douglas, T. B. and King, E. G. (1968) *High-temperature drop calorimetry*. In J. P. McCullough and D. W. Scott, Eds., *Experimental Thermodynamics, Vol. 1, Calorimetry of Nonreacting Systems*, p. 293-331. Plenum Press, New York.
- Eggert, R. G. and Kerrick, D. M. (1981) *Metamorphic equilibria in the siliceous dolomite system: 6 kb experimental data and geologic implications*. *Geochimica et Cosmochimica Acta*, 45, 1039-1049.
- Goldsmith, J. R. and Graf, D. L. (1958) *Relation between lattice constants and composition of the Ca-Mg carbonates*. *American Mineralogist*, 43, 84-101.
- Goldsmith, J. R., Graf, D. L., and Heard, H. C. (1961) *Lattice constants of the calcium-magnesium carbonates*. *American Mineralogist*, 46, 453-457.
- Graf, D. L. and Goldsmith, J. R. (1955) *Dolomite-magnesian calcite relations at elevated temperatures and CO₂ pressures*. *Geochimica et Cosmochimica Acta*, 7, 109-128.
- Greenwood, H. J. (1963) *The synthesis and stability of anthophyllite*. *Journal of Petrology*, 4, 317-351.
- Haas, J. L., Jr. and Fisher, J. R. (1976) *Simultaneous evaluation and correlation of thermodynamic data*. *American Journal of Science*, 276, 525-545.
- Jacobs, G. K., Kerrick, D. M., and Krupka, K. M. (1981) *The high-temperature heat capacity of natural calcite (CaCO₃)*. *Physics and Chemistry of Minerals*, 7, 55-59.
- Krupka, K. M. (1984) *Thermodynamic Analysis of Some Equilibria in the System MgO-SiO₂-H₂O*. Ph.D. Thesis, The Pennsylvania State University, University Park.
- Krupka, K. M., Robie, R. A., and Hemingway, B. S. (1979) *High-temperature heat capacities of corundum, periclase, anorthite,*

- $\text{CaAl}_2\text{Si}_2\text{O}_8$ glass, muscovite, pyrophyllite, KAlSi_3O_8 glass, grossular, and $\text{NaAlSi}_3\text{O}_8$ glass. *American Mineralogist*, 64, 86–101.
- Krupka, K. M., Robie, R. A., Hemingway, B. S., Kerrick, D. M., and Ito, J. (1985) Low-temperature heat capacities and derived thermodynamic properties of anthophyllite, diopside, enstatite, bronzite, and wollastonite. *American Mineralogist*, 70, 249–260.
- Leonidov, V. Ya. and Khitarov, N. I. (1967) New data on the thermodynamic properties of talc. *Geokhimiya*, 1044–1049 (transl. *Geochemistry International*, 4, 944–949, 1969).
- Maier, C. G. and Kelley, K. K. (1932) An equation for the representation of high-temperature heat content data. *Journal of the American Chemical Society*, 54, 3243–3246.
- McAdie, H. H., Garn, P. D., and Menis, O. (1972) Standard reference materials: Selection of differential thermal analysis temperature standards through a cooperative study (SRM 758, 759, 760). National Bureau of Standards Publication 260–40.
- McKinstry, B. and Skippen, G. (1978) An experimental study of the stability of tremolite. (abstr.) Geological Society of America, Abstracts with Program, 10, 454.
- Rabbitt, J. C. (1948) A new study of anthophyllite series. *American Mineralogist*, 33, 263–323.
- Rayner, J. H. and Brown, G. (1966) Triclinic form of talc. *Nature*, 212, 1352–1353.
- Rayner, J. H. and Brown, G. (1973) The crystal structure of talc. *Clays and Clay Minerals*, 21, 103–114.
- Robie, R. A. and Stout, J. W. (1963) Heat capacity from 12 to 305° K, and entropy of talc and tremolite. *Journal of Physical Chemistry*, 67, 2252–2256.
- Robie, R. A., Hemingway, B. S., and Fisher, J. R. (1979) Thermodynamic properties of minerals and related substances at 298.15 K and one bar (10^5 pascals) pressure and at higher temperatures. U.S. Geological Survey Bulletin 1452.
- Ross, M., Smith, W. L., and W. H. Ashton (1968) Triclinic talc and associated amphiboles from Gouverneur mining district, New York. *American Mineralogist*, 53, 751–769.
- Roth, W. A. and Bertram, W. W. (1929) Measuring the specific heats of metallurgically important materials through a large range of temperature with the aid of two new types of calorimeters. *Zeitschrift für Elektrochemie*, 35, 297–308.
- Slaughter, J., Kerrick, D. M., and Wall, V. J. (1975) Experimental and thermodynamic study of equilibria in the system $\text{CaO-MgO-SiO}_2\text{-H}_2\text{O-CO}_2$. *American Journal of Science*, 275, 143–162.
- Southard, J. C. (1941) A modified calorimeter for high temperatures. The heat content of silica, wollastonite and thorium dioxide above 25°. *Journal of the American Chemical Society*, 63, 3142–3146.
- Stout, J. W. and Robie, R. A. (1963) Heat capacity from 11 to 300° K, entropy, and heat of formation of dolomite. *Journal of Physical Chemistry*, 67, 2248–2252.
- Thompson, A. B., Perkins, D., III, Sonderegger, U. and Newton, R. C. (1978) Heat capacities of synthetic $\text{CaAl}_2\text{SiO}_6\text{-CaMgSi}_2\text{O}_6$ pyroxenes. (abstr.) EOS (Trans. American Geophysical Union), 59, 395.
- von Gronow, H. E. and Schwierte, H. E. (1933) Die spezifischen Wämen von CaO , Al_2O_3 , $\text{CaO}\cdot\text{Al}_2\text{O}_3$, $3\text{CaO}\cdot\text{Al}_2\text{O}_3$, $2\text{CaO}\cdot\text{SiO}_2$, $3\text{CaO}\cdot\text{SiO}_2$, $2\text{CaO}\cdot\text{Al}_2\text{O}_3\cdot\text{SiO}_2$ von 20 bis 1500 C. *Zeitschrift für Anorganische und Allgemeine Chemie*, 216, 185–195.
- Wagner, V. H. (1932) Zur thermochemie der metasilikate des calciums und magnesiums und des diopsids. *Zeitschrift für Anorganische und Allgemeine Chemie*, 208, 1–22.
- White, W. P. (1919) Silicate specific heats. Second series. *American Journal of Science*, XLVII, 1–43.

*Manuscript received, December 7, 1983;
accepted for publication, November 19, 1984.*